Available online at www.sciencedirect.com
SCIENCE DIRECT
Catalysis Today 110 (2005) 76–85
CATALYSIS TODAY
www.elsevier.com/locate/cattod

Kinetic investigations on methanol steam reforming on PdZn catalysts in microchannel reactors and model transfer into the pressure gap region

P. Pfeifer *, A. Kölbl, K. Schubert

Institute for Micro Process Engineering, Forschungszentrum Karlsruhe, Hermann-von-Helmholtz Platz 1, 76344 Eggenstein-Leopoldshafen, Germany

Available online 19 October 2005

Abstract

In the present study, a microchannel reactor was used in an integral mode of reactor operation to investigate parameter influences on the steam reforming of methanol on PdZn catalysts prepared by washcoating the microchannels with ZnO nanoparticles. Different models derived from significant concentration parameters were evaluated concerning their suitability to describe the kinetics of the methanol reforming reaction in the examined parameter range. Water gas shift reaction was found to be negligible in the reaction network. Methanol decomposition, even though it was influenced by the reactor material, was neglected for the modelling since CO was present only at a minor extent at the reactor outlet. Superior isothermal behaviour of the microchannel reactor is supposed to be responsible for good correlations of the derived models with experimental results. One of the models, the ''global model'', was transferred to results from experiments in the pressure gap region obtained in a similar microchannel reactor suitable for low-pressure application. Although this was a model extrapolation, model and experiment were in good accordance for a wide range of absolute and methanol partial pressures, molar ratios of water to methanol and temperatures.

Keywords: Methanol steam reforming; Microstructured/microchannel reactor; Kinetics; PdZn alloy; Pressure gap; Washcoat

1. Introduction

The reaction of water and methanol on copper was first published in 1921 [1]. Christiansen observed hydrogen and carbon dioxide in a molar ratio of 3/1 together with minor traces of carbon monoxide. Copper based catalysts are the most widely used catalyst for the steam reforming of methanol. Beside them PdZn alloy catalysts are gaining interest in chemical research and industrial application [2].

While Palladium is predominantly producing CO and H_2 (methanol decomposition), the activity and selectivity towards CO_2 is enhanced when using ZnO as carrier material. The reason therefore is obviously the interaction of palladium and zinc [3]. Activity and selectivity can further be enhanced with prior reduction of the catalytic material in a hydrogen stream. Due to the formation of a PdZn alloy, which can be indicated by X-ray diffraction, X-ray photoelectron spectroscopy and auger electron spectroscopy [4–6], similar catalytic activity compared to copper catalysts is achieved.

In early works on the mechanism of methanol steam reforming [7–10] a mechanism starting with the decomposition of methanol, which is followed by the water gas shift reaction was proposed. This idea has been disproved, since the amount of CO in the product gas composition should decrease when increasing residence time. In fact, the amount of carbon monoxide is rising, when increasing residence time [3,11].

An alternative mechanism including methyl formate as intermediate has been proposed in 1981 by Takezawa and co-workers [12]. In works of Trimm and co-workers [13–15], it is shown, that the rate of the overall reaction is approximately the rate of the formation of methyl formate in the absence of water. It was concluded, that the rate determinant step of the overall reaction is part of the formation of methyl formate and not part of the decomposition of methyl formate to carbon monoxide and hydrogen. The activation energy for methanol dehydrogenation to methyl format was ascertained to 103 kJ/mol. This is approximately the same value, which was given for the overall process (105 kJ/mol). Other proposed intermediates are adsorbed methoxy species, which react to adsorbed

* Corresponding author. Tel.: +49 7247 82 4767; fax: +49 7247 82 3186.
E-mail address: peter.pfeifer@imvt.fzk.de (P. Pfeifer).
URL: www.fzk.de/imvt-en

0920-5861/$ – see front matter © 2005 Elsevier B.V. All rights reserved.
doi:10.1016/j.cattod.2005.09.014

Nomenclature

$a1$	methanol exponent
$a2$	hydrogen exponent
c	speed of light (m/s)
c_i	concentration of gas component i (mol/m^3)
c_{H_2}	hydrogen concentration (mol/m^3)
c_{Me}	methanol concentration (mol/m^3)
E_A	activation energy (kJ/mol)
E_v	vibration energy (J)
ΔE_v	difference in vibration energy (J)
h	Planck's constant (J s)
$\Delta H_{H_2,Des}$	hydrogen desorption enthalpy (kJ/mol)
$\Delta H_{Me,Ads}$	methanol adsorption enthalpy (kJ/mol)
k	Boltzmann's constant (J/K), pre-exponential factor (volume specific) ((mol/m^3)$^{1-a1-a2}$/s)
k_S	surface reaction constant (volume specific) (mol/m^3 s)
$K_{H_2,Des}$	hydrogen desorption equilibrium constant (mol/m^3)
$K_{Me,Ads}$	methanol adsorption equilibrium constant (m^3/mol)
k^*	pre-exponential factor (volume specific) at T^* ((mol/m^3)$^{1-a1-a2}$/s)
$K^*_{H_2,Des}$	hydrogen desorption equilibrium constant at T^* (mol/m^3)
$K^*_{Me,Ads}$	methanol adsorption equilibrium constant at T^* (m^3/mol)
$m_{catalyst}$	catalyst mass (g)
r	reaction rate (volume specific) (mol/m^3 s)
$r_{m,j}$	catalyst mass specific reaction rate (mol/g$_{catalyst}$ s)
r_S	surface reaction rate (volume specific) (mol/m^3 s)
$r_{V,j}$	volume specific reaction rate (mol/m$^3_{channels}$ s)
$R_{methanol}$	volume specific methanol consumption rate (mol/m^3 s)
$R_{D\text{-}Methanol}$	integral D-methanol consumption rate (mol/g$_{catalyst}$ s)
$R_{Methanol}$	integral methanol consumption rate (mol/g$_{catalyst}$ s)
T	reaction temperature (K)
T^*	reference temperature (K)
$\bar{u}$	mean gas velocity in the channel (m/s)
v	quantum number
$V_{reactor}$	reactor (uncoated channel) volume (m^3)
z	reaction coordinate in axial channel direction (m)

Greek symbols

λ	wavelength of vibration (m)
μ	reduced atomic mass (kg)
θ_{free}	degree of surface sites free for adsorption
θ_H	degree of surface sites with hydrogen adsorbed
θ_{Me}	degree of surface sites with methanol adsorbed
ν	vibration frequency (s^{-1})
$\nu_{i,j}$	stoichiometric factor
Ω	force constant (N/m)

formaldehyde. Peppley et al. identified methoxy and formate species in DRIFTS studies [16]. No indication for the presence of methyl formate is given in these studies.

The role of methyl formate as proposed intermediate is yet not clear. For copper catalyst Takahashi et al. [17] proposed, that the mechanism includes methyl formate at high temperatures, while at low temperatures no methyl formate is included in the mechanism of methanol steam reforming.

2. Experimental

2.1. Catalyst preparation

The PdZn catalyst used in this study was prepared on microstructured foils by the use of a washcoating procedure with ZnO nanoparticles.

The microstructured foils were made of an aluminium alloy with 3 wt.% magnesia (150 μm thickness, melting point 660 °C). Every foil had 80 straight channels with a cross-section of 100 μm × 100 μm with fins of 50 μm thickness in between the channels.

The washcoating procedure includes the following preparation steps:

1. Impregnation of ZnO nanoparticles (Nanophase Inc.) with a saturated solution of palladium acetate ($PdAc_2$) in toluene, i.e. evaporation of toluene from the stirred nanoparticle slurry containing ZnO in the palladium acetate solution at 60 °C and 200 mbar. The desired loading of ZnO with pure Pd is 10 wt.% (mass palladium per catalyst, i.e. mass of palladium plus ZnO).
2. Drying of $PdAc_2$/ZnO at 90 °C for 24 h.
3. Pre-calcination (Calcination 1) at 250 °C for 2 h, heating up at a rate of 4 K/min in a vented muffle furnace to obtain Pd/ZnO.
4. Dispersing the Pd/ZnO in an aqueous solution of hydroxy ethyl cellulose (HEC) (Merck). No data about molecular weight of the polymer was available. The weight content of cellulose was 1% in water. The amount of particles in the slurry was 20 wt.%. Dispersing was done with a magnetic stirrer at a stirring speed of 1100 min^{-1} for 24 h.
5. Application of the slurry to the microstructured foils (washcoating), i.e. filling the channels with slurry and drying at room temperature subsequently. Normally three cycles of filling and drying had to be carried out to obtain a loading of 20 wt.% catalyst per final foil weight (after further calcining) which is equal to a final layer thickness of approximately 20 μm in the channels.
6. Calcination (Calcination 2) of the coated foil at 450 °C for 5 h, heating up at a rate of 4 K/min, in a tube furnace at an air flow of 300 ml/min STP to obtain complete polymer burn off and sintering of the particles to form an adhesive layer. Details about the sintering behaviour can be found in an earlier publication [18].
7. Reduction of the palladium and of the necessary amount of ZnO to form the active phase, i.e. PdZn alloy, in a tube furnace under a flow of 2 l/min STP of 1 vol.% H_2 in argon at 500 °C for 5 h, heating up at a rate of 4 K/min.

More details about the preparation and its influence on the catalytic properties can be found in a previous publication [19]. Information about the homogeneity of the obtained layers were published recently [20].

2.2. Test conditions

Two different experimental setups were applied for determination of the kinetics of methanol steam reforming on PdZn at absolute pressures above 1 bar and for the pressure gap region (below 1 bar). Details about the setups for the experiments can be found elsewhere [18,21].

The major differences between the two test rigs concerned the dosing concept, the reactor and tube sealing and the analytics. For low pressures it was necessary to have enhanced leak tightness and very small mass flows to keep residence times comparable. The reactor sealing was therefore changed from graphite to a metallic copper ring for the low-pressure experiments. For the analytics of the product gas composition a mass spectrometer (Balzers Prisma QMS 200) was applied instead of gas chromatography (Chrompack Micro-GC) at higher pressures. Finally dosing of methanol and steam was done by the use of two saturators for the low-pressure experiments. In this case the flow was controlled by pressure drop measurements over capillaries; a concept which allowed using only small amounts of the generated vapour streams.

The investigated parameter range due to restrictions of the experimental setup are given below. The standard experimental conditions (when nothing else is given in the figure captions these values are valid) are represented in bold letters.

1. Elevated pressure experiments: **3** and 6 bar total pressure, **18** and 36 ml/min helium at STP for standard methanol and water flow without product co-feeding (values are slightly different when using other reactant concentrations to ensure constant residence time), 0.13–0.45 (**0.29**) g/h methanol flow, 0.24–0.40 (**0.32**) g/h water flow, two microstructured foils stacked in the reactor, foil/channel length 16/32/**64** mm, catalyst layer thickness 5–**20** μm; residence time 0.0625–**0.25** s (referring to uncoated channels at 250 °C and total pressure), reaction temperature 210–285 °C.
2. Low pressure experiments: **1** bar–30 mbar total pressure, inlet partial pressure of 0.6–200 mbar (**50**), water to methanol molar ratio = 1/1. Argon as carrier gas. Six microstructured foils stacked in the reactor, foil/channel length 60 mm, catalyst layer thickness 20 μm; residence time 0.2 s (referring to uncoated channels at 250 °C and total pressure), reaction temperature 210–330 °C.

3. Results and discussion

3.1. Boundary conditions

Preliminary to catalytic runs for parameter study every catalyst had to be treated by a series of temperature ramps in the desired reaction temperature range until they reached a stable methanol conversion and selectivity curve for methanol steam reforming. The catalysts examined in the different experimental setups were not identical but prepared under the same conditions. This might be also a reason for different deactivation extent. Other reasons for this could be the different limits in partial pressures of reactants and different maximum reaction temperatures. For low-pressure experiments, it was quite obvious that deactivation time/number of cycles exceeded that of the experiments on fresh catalysts at elevated pressure due to a lower amount of methanol converted per time. However, the activity remained higher when the stable phase was reached for the experiments at elevated pressure. During parameter study, a temperature ramp at standard conditions was used in intervals to ensure catalyst stability.

Conversion of methanol and byproduct formation on uncoated microstructured aluminium foils and on ZnO coated foils as well as in the empty test reactors, where the microstructured foils where clamped for the present study, were found to be negligible under all conditions.

Catalyst loss during experiments was examined by weighing of the samples before and after tests. No obvious catalyst loss was found there.

Considering isothermal operation of the reactor, it was proven that no axial temperature gradient in the test reactor or in the gas phase between the inlet and outlet was present experimentally. Calculations (see also [22]) about heat sink and supply taking into account the heat conductivity of the catalyst layers and the microstructured elements confirmed also no gradients.

The assumption of flow continuum mechanics in the microchannels is valid at least for the elevated pressure experiments as Knudsen numbers were calculated to be lower than 0.001. For low-pressure experiments this validation is difficult, since Knudsen number is increasing fast. A validation is assumed to be possible by indirect argumentation via successful model transfer (see later).

Influence of the channel inlet to the flow regime in the channel was negligible as the ratio of channel length to channel diameter was in all cases greater than 100.

Although the flow in microchannels under the examined conditions is laminar, the assumption of plug flow in the reactor was proven to be valid from simulations and from use of estimation methods of the Bodenstein number. The simulation of a hydrogen breakthrough in a helium stream at near standard conditions in the reactor was transferred to a Bodenstein number of 150–200. A similar value of 166 was estimated by standard equations [23,24]. Experimental determination was not successful as the applied mass spectrometer with capillary inlet had a very low Bodenstein number itself.

The pressure drop in the coated channels was measured at room temperature applying 200 ml/min air (STP) to a two microstructured foil system with 20 μm catalyst coating to calculate the free cross-section of the coated channels and to subsequently estimate the pressure drop in the real reaction mixture. The pressure drop in air was 0.32 bar, which is about 10% of the lowest total pressure in the setup for elevated pressure experiments. As far as the velocity at the applied flow

(200 ml/min) is an order of magnitude higher than under reaction conditions and viscosity of air is higher than the helium based mixture, one can neglect the pressure drop (below 10 mbar depending on the conversion degree) when modelling the reaction network.

3.2. Mass transfer limitation

Conventional tests for mass transfer limitation to the catalyst bulk, i.e. varying fluid velocities to reduce the thickness of the laminar boundary flow around the catalyst particle (or catalyst layer), are not applicable to microchannels. The overall flow itself is laminar (small Reynolds numbers) in most cases. Consequently, the absence of mass transfer limitation for the overall reaction rate has been examined by varying diffusion coefficients. This has been carried out in two different ways.

(1) Variation of the total pressure [21] (in the setup for low pressure measurements) at constant reactant inlet partial pressures and residence times.
(2) Change of the carrier gas [21,25] (in the setup for low pressure measurements and in the setup for high pressure measurements) at constant reactant inlet partial pressures and residence times.

Since no change in catalytic activity, i.e. conversion degree, has been observed, mass transport limitation from the gas to the porous catalyst layer has been ruled out.

The variation of the diffusion coefficient in the reactant mixture can also be applied for the examination of the absence of mass transport limitation in the porous catalyst layer (the catalyst having pore sizes in the range 50–100 nm). In order to validate the absence of pore diffusion limitation with additional experiments, the catalyst layer thickness was varied in the setup for elevated pressure from 5 to 20 μm in steps of around 5 μm (due to an increase in preciseness of analysis the catalyst mass was determined experimentally).

Although the residence times decreases to around 60% when increasing the layer thickness (catalyst mass) from 5 to 20 μm, the conversion degree at a constant reaction temperature showed nearly a linear relation to the catalyst mass. With the knowledge of a decreasing reaction rate with increasing conversion degree this linearity is a strong argument for absence of pore diffusion limitation for the overall reaction rate.

3.3. Reaction network

In literature, three reactions are considered to be relevant in the methanol steam reforming, i.e. steam reforming (SR Eq. (1)), decomposition (DC, Eq. (2)) and reverse water gas shift (RWGS, Eq. (3)):

$$CH_3OH + H_2O = CO_2 + 3H_2 \quad (1)$$

$$CH_3OH = CO + 2H_2 \quad (2)$$

$$CO_2 + H_2 = CO + H_2O \quad (3)$$

The assumption for PdZn as well as for copper systems is that steam reforming is the most relevant reaction in the system. This can be proven by experiments with different residence times and by comparison of measured and calculated equilibrium CO concentrations. The calculated values of carbon monoxide have to be obtained from equilibrium of the RWGS reaction using the measured CO_2, H_2O, H_2 and methanol concentrations. If the calculated concentration CO_{eq} is higher than the experimental concentrations CO_{exp}, one can conclude that CO is no intermediate, i.e. CO is produced by RWGS reaction. From data already published [19] (elevated pressure experiments) we also believe that hydrogen production is dominantly conducted by steam reforming. However, at low reaction temperatures the measured CO value is sometimes far above the equilibrium CO value. This includes measurements at different residence times where residence time was varied by different foil lengths of 16, 32 and 64 mm. The absolute CO concentration remained independent of the foil length (Fig. 1) in the pressure setup at standard conditions, i.e. constant overall inlet flow and concentrations. Also CO or CO_2 co-feeding (range up to 0.65 vol.% CO or 7.5 vol.% CO_2), which should influence the equilibrium of the water gas shift reaction, did not influence the CO and CO_2 selectivities (co-feed subtracted) at constant residence time. From these both observations, we assume that methanol decomposition is a parallel reaction and that water gas shift is negligible in the reaction network.

The high CO concentration values for the coated micro-structured foils at low temperatures are expected to be a result of the foil-catalyst interaction since PdZn gets into contact also with aluminum of the foil. Even though the interaction is not directly accessible by spectroscopic methods, this assumption is supported by switching the impregnation and coating steps during the catalyst procedure (pre- and post-impregnation) as well as by results from powder catalysts, where CO_2 selectivity increased from post- to pre-impregnation (pre-impregnation is identical to the preparation used in this study) and increased furthermore to powder catalyst (pre-impregnation with no application to foils). The powder catalyst exhibited lower

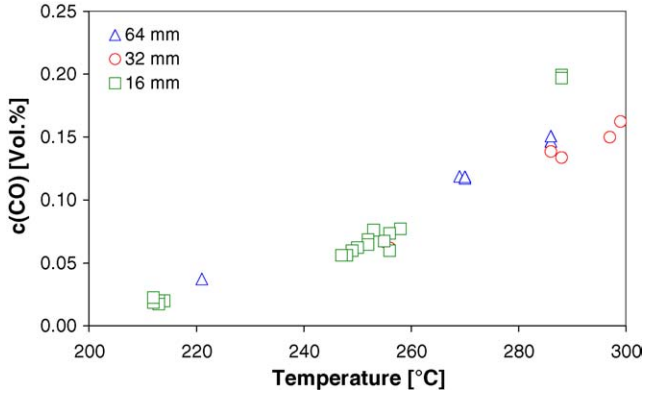

Fig. 1. CO concentration at the reactor outlet vs. reaction temperature for different catalyst foil lengths.

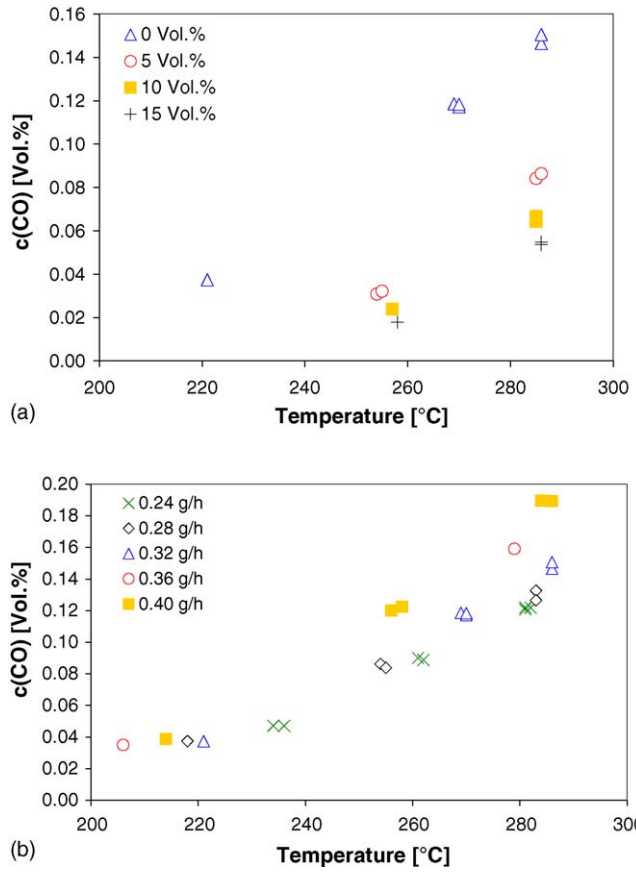

Fig. 2. CO concentration at the reactor outlet vs. reaction temperature for (a) different concentrations of hydrogen addition to the reactor feed and (b) for different water inlet feed at constant residence time.

measured CO concentration than equilibrium CO values all over range of reaction temperature [19].

In this study, more experiments were conducted to find also the parameter influences on the CO formation from the parameters of reactant composition. Fig. 2a shows a suppression of CO formation with hydrogen co-feeding into the reactor (maximum 15 vol.% H_2; carrier gas flow reduced by the amount of co-flow as mentioned in Section 2). The hydrogen decreases the measured CO concentration to a value below the CO water gas shift equilibrium concentration over the whole reaction temperature examined. Another parameter which influences the water gas shift equilibrium is the water content in the reactor feed. Increasing water concentration in the steam to carbon ratio of 1.4–2.5 led to an increase in measured CO concentration while $CO_{eq.}$ gets smaller (Fig. 2b). This is an opposite trend to what was expected to happen – even at that high steam to carbon ratio. However, as water gas shift and reverse water gas shift were found to be negligible and CO is produced by decomposition of methanol, a possible reason for this behaviour might be the influence of the reaction gas mixture on catalyst phase to be present at the reactor inlet. Whereas hydrogen co-feed leads to an increase in reduced palladium phases and water acts as oxidant, CO formation might also be affected by oxidation state of palladium. Methanol inlet concentration did not influence the CO-value during experiments.

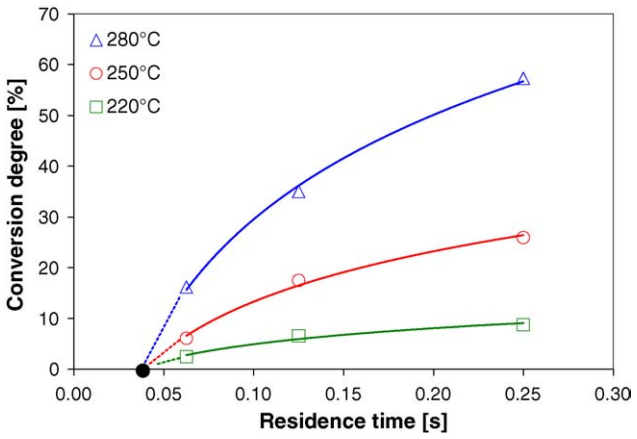

Fig. 3. Conversion degree of methanol at different reaction temperatures vs. residence time (different foil length at constant overall inlet flow).

3.4. Significant parameters

Significant parameters for the reforming were examined in the following section only for the steam reforming reaction as CO formation was always less than 5% CO selectivity and therefore negligible. Another reason why CO was not subject for the modelling is an experimental one. Analytics allowed only a CO measurement approximately every 20th GC run, thus loading of the molsieve column of the micro GC with water, methanol and CO_2.

The variation of the residence time according to the experiments in Section 3.3 highlighted a reduction of conversion by a reduction of the catalytic coated foil length all over the reaction temperature range examined. Fig. 3 shows the conversion degree as a function of residence time. When trying to fit the data at constant reaction temperature, it could be concluded that no conversion takes place at a residence time below 0.04 s. This could be true if there was an induction period for the reaction, i.e. formation of hydrogen by decomposition and subsequent reduction of palladium phases for methanol steam reforming. A more reasonable explanation is a bypass in the reactor compartment. It was tried to minimise the bypass by varying stack height (different thickness of unstructured foils on top of the two foil stack). However, in different measurements at conditions (high temperature) where near 100% conversion should be expected, a maximum bypass along the foils of 10% is estimated. The s-shaped curve of the conversion degree versus reaction temperature reached a level of only 90–96% asymptotically. Thermal expansion of the materials during temperature ramps is supposed to result in gaps between foils and reactor compartment. A gap of 15 μm could lead to up to 10% bypass according to pressure drop calculations.

The study of significant concentration parameters was started with the influence of product gases on the yield of CO_2. Whereas CO and CO_2 did not influence the conversion or the selectivity, again hydrogen co-feeding reduced the conversion significantly. This reduction was not as high as for the CO concentration (see Fig. 4).

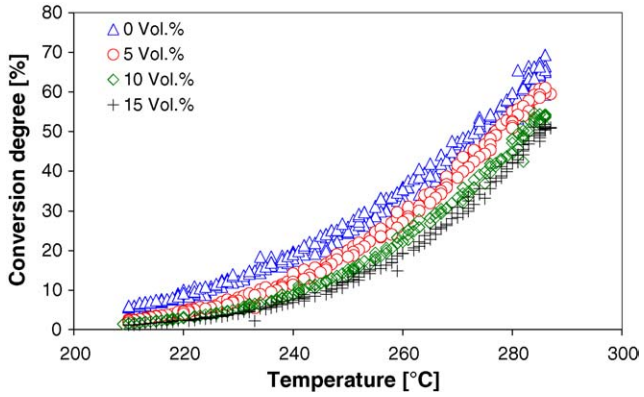

Fig. 4. Conversion degree of methanol depending on the hydrogen addition at the reactor inlet as a function of reaction temperature.

Methanol and water concentrations were varied separately. For conversion the methanol influence was visible (Fig. 5) whereas water had no influence. The comparison of Fig. 5a and b shows that increasing the inlet concentration of methanol leads to reduction of conversion but the molar flow of methanol converted increases. Having in mind the negative influence of the product hydrogen methanol has definitely a positive order considering a potential rate equation.

Trace amounts of dimethyl ether (DME) were found in the reaction system (up to 60 ppm), which were only dependent on

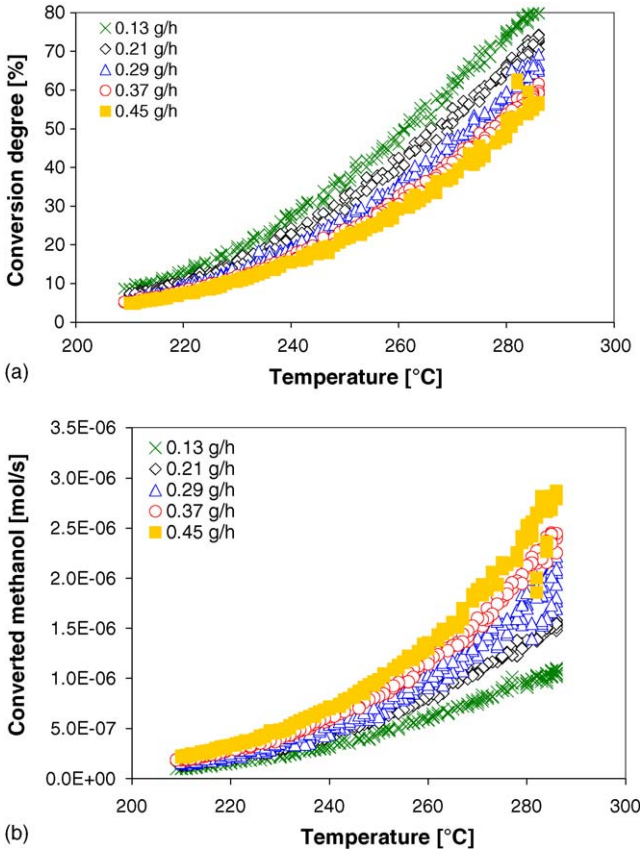

Fig. 5. (a) Conversion degree of methanol and (b) converted methanol as a function of reaction temperature for different methanol inlet flows at constant residence time and constant water flow.

the water and methanol concentration. The influence of both parameters had a direct correlation with the increase in DME equilibrium concentration when increasing methanol partial pressure or a decrease of DME equilibrium concentration when increasing the water partial pressure.

3.5. Intermediate products and rate determining step

The following section deals with the intermediate product methyl formate and experimental studies concerning the rate determining step in methanol steam reforming using the isotope CD_3OD (four times deuterium D = ^{2}H). Both experimental studies were conducted in the low-pressure setup for experimental circumstances (exchangeability of reactants and isotopic analysis) at 1 bar total pressure.

A comparison of the integral molar consumption rate of methyl formate and methanol per mass of catalyst showed that the rate of the methyl formate consumption is only twice that of methanol consumption.

Considering reaction rates of methyl formate over copper in literature [14], i.e. pre-exponential factor and activation energy of both reactions, the methyl formate reaction should be 420 times faster than methanol reaction. This is a strong hint that methyl formate is not an intermediate in methanol reforming over the PdZn catalyst as assumed by Takahashi et al. [17]. The absence of methyl formate in the reaction mechanism is also supported by DRIFTS studies [25] where adsorption of methyl formate on PdZn was not obvious.

Isotopic experiments were conducted with a 1:1 mixture of natural and isotopic methanol (D-methanol) to compare the conversion of both substances in one step (Fig. 6a). Because it was experimentally verified that deuterium is shifted in the molecular mixture to equal ratio in the O–H bond, a difference of the conversion degrees cannot have an origin in the O–H bond breakage. A C–H bond breakage has to be rate determining. This is an experimental hint for the assumed analogy of copper and PdZn systems made earlier in literature [26,27].

To obtain additional information about the significance of the above statement considering the C–H bond breakage an estimation was made referring to force constant of the bond (Ω), vibration energy (E_v) and integral methanol consumption rate (R) depending on the difference in vibration energy (ΔE_v) with the following equations:

$$\Omega = \mu\left(\frac{2\pi c}{\lambda}\right)^2 \tag{4}$$

$$E_v = \frac{v + 0.5}{h\nu} \quad \text{with} \quad \nu = \frac{(\Omega/\mu)^{0.5}}{2\pi} \tag{5}$$

$$\frac{R_{\text{Methanol}}}{R_{\text{D-Methanol}}} = e^{-(\Delta E_v/kT)} \tag{6}$$

where, c represents the speed of light, λ the wavelength of the vibration, v the quantum number of vibration (first order = 0), h the Planck's constant, μ the reduced atomic mass, ν the

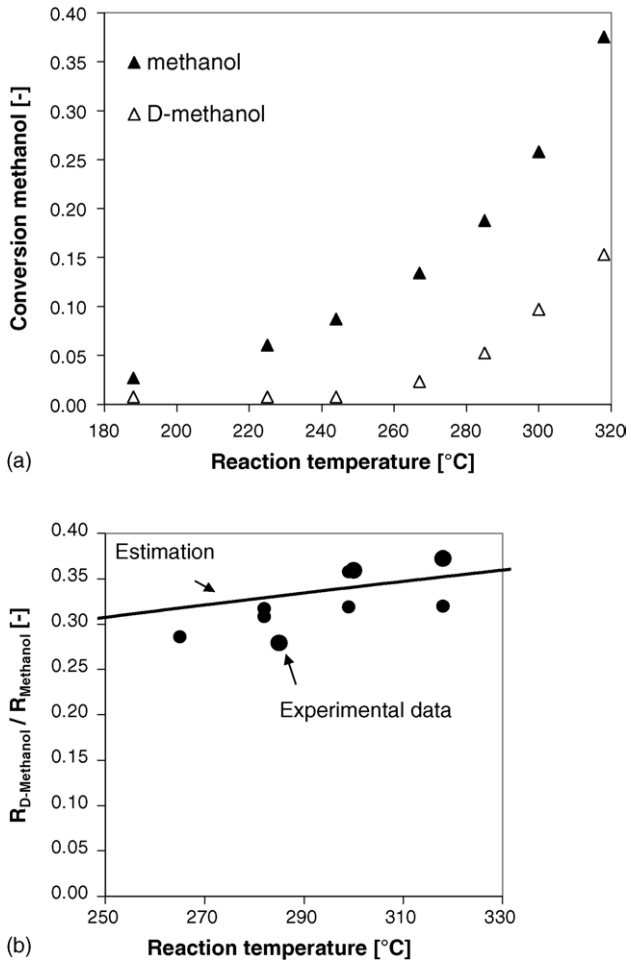

Fig. 6. (a) Comparison of methanol and D-methanol conversion degree and (b) experimental isotope consumption ratio in comparison to estimated isotope consumption ratio (from vibration energy) as a function of reaction temperature in 1:1 mixture of methanol and D-methanol.

vibration frequency, k the Boltzmann's constant and T is the reaction temperature.

For the C–H bond a vibration wave number of 2982 cm^{-1} was used from DRIFTS studies [25] to calculate the theoretical curve of the R ratio depending on the reaction temperature. The comparison (Fig. 6b) shows a good accordance of measured and estimated values verifying the significance of the difference of the conversion degrees of D– and natural methanol to a C–H bond breakage.

3.6. Models and parameter estimation

The obtained experimental data from elevated pressure and from hints about the rate-determining step (RDS) at 1 bar in the low-pressure setup were used to derive mathematical rate models and model discrimination.

gPROMS© was applied for parameter estimation by integration of concentration curves along the reaction axis by applied least squares method. A 100 reactor segments were used to do the integration. To reduce correlations during estimation a reference temperature of 563 K was introduced. All data obtained at this temperature are marked with an asterisk (*). The increase in gas velocity due to volume expansion at enhanced conversion degrees was considered at every new segment depending on hydrogen partial pressure and a temperature-dependent velocity was calculated for every reaction temperature. For mass balance of the reactor, a semi-homogeneous statement of the channels was made assuming a plug flow reactor (plug flow assumption see Section 3.1). This also involves the assumption that neither mass transfer limitation is obvious in the channel (limitation by diffusion to the catalyst layer) nor in the catalyst layer (pore diffusion limitation; see Section 3.2). An axial dispersion was introduced in the model with a $D_{ax} = 10^{-10}$ m^2/s to increase the solubility of the differential equation at the boundary of the segments without influence on the solution itself (Eq. (7)).

$$0 = -\bar{u}\frac{dc_i}{dz} - c_i\frac{d\bar{u}}{dz} + D_{ax}\frac{d^2c_i}{dz^2} + \sum_j \nu_{i,j} r_{V,j} \tag{7}$$

For all experiments conducted with a 20 μm layer, the volumetric rate expressions can be transferred into catalyst mass specific ones by the following equation:

$$r_{m,j} = \frac{r_{V,j} V_{reactor}}{m_{catalyst}} \tag{8}$$

with a ratio $m_{catalyst}/V_{reactor} = 976$ kg/m^3.

Three models derived from solubility with a good match of experimental and model concentrations: a potential rate expression, a global hyperbolic rate expression and hyperbolic rate expression with knowledge of the RDS of Section 3.5.

The potential rate expression:

$$-R_{methanol} \equiv r = k c_{Me}^{a1} c_{H_2}^{a2} \tag{9}$$

considers a methanol and hydrogen influence on the conversion/methanol reforming yield.

The global hyperbolic rate expression:

$$-R_{methanol} \equiv r_s = \frac{k_s K_{Me,Ads} c_{Me}}{(1 + K_{Me,Ads} c_{Me} + \sqrt{c_{H_2}/K_{H_2,Des}})^6} \tag{10}$$

is similar in terms of methanol and hydrogen influences. However, it assumes the influence of these components by methanol adsorption and hydrogen desorption which are competing. Rate-determining step is the surface reaction in total (Eq. (12)):

$$CH_3OH + z \rightleftharpoons CH_3OH - z \tag{11}$$

$$CH_3OH - z + (H_2O) \rightleftharpoons 6H - z + (CO_2) \quad \text{(RDS)} \tag{12}$$

$$2H - z \rightleftharpoons H_2 + z \tag{13}$$

The different adsorption sites z or i.e. their utilisation degrees θ are eliminated in the rate expression by using the fact that the sum of the utilisation degrees is 1.

The third rate expression:

$$-R_{\text{methanol}} \equiv r_s = \frac{k_s K_{\text{Me,Ads}} c_{\text{Me}}}{\left(1 + K_{\text{Me,Ads}} c_{\text{Me}} + \sqrt{c_{\text{H}_2}/K_{\text{H}_2,\text{Des}}}\right)^3} \quad (14)$$

considers even more the microkinetic steps of the surface reaction which are given by the following equations:

$$\text{CH}_3\text{OH} + z \rightleftharpoons \text{CH}_3\text{OH} - z \quad (15)$$

$$\text{CH}_3\text{OH} - z + 2z \rightleftharpoons \text{HCHO} - z + 2\text{H} - z \quad (\text{RDS}) \quad (16)$$

$$\text{HCHO} - z + 2z + (\text{H}_2\text{O}) \rightleftharpoons \text{HCOOH} - z + 2\text{H} - z \quad (17)$$

$$\text{HCOOH} - z + z \rightleftharpoons 2\text{H} - z + (\text{CO}_2) \quad (18)$$

$$2\text{H} - z \rightleftharpoons \text{H}_2 + z \quad (19)$$

For the elimination of the utilisation degrees of the adsorption sites the degrees with formaldehyde and acetic acid are neglected (fast reactions), i.e.

$$\theta_{\text{Me}} + \theta_{\text{H}} + \theta_{\text{free}} \approx 1 \quad (20)$$

The results from parameter estimation are given in Table 1 for the different models. The calculated values for the activation energy of 114.4 kJ/mol (RDS based model) is near the values of 113 kJ/mol (PdZn 111) [28] and 107 kJ/mol (PdZn100) [29], calculated by theoretical chemists by means of ab-initio methods for the proposed rate determining step, the C–H bond breakage from the adsorbed methoxy species.

Similarities of the PdZn catalyst in this study and copper systems are obvious from the exponential model. The methanol exponent for PdZn is 0.66 (0.564–0.63 for the copper system [30–32]). The hydrogen influence seems to be more pronounced as the exponent is often higher than that for copper systems (0 to −0.23 [31,32]; only once a value as high as −0.647 has been reported [30]). Water with a negligible influence on PdZn activity, however, seems to be important for copper (0.39–0.4 [31,32]). This influence was found also within a PdZn study [33]. Nevertheless, in the latter publication a

Table 1
Estimated model parameters and their deviation

Model	Parameter	Value	Deviation
Exponential model	E_A (kJ/mol)	123.1	0.06
	k^* ((mol/m^3)$^{1-a1-a2}$/s)	31.1	0.04
	$a1$	0.66	0.06
	$a2$	−0.53	0.07
Global model	E_A (kJ/mol)	105.5	0.02
	k_S^* (mol/m^3 s)	2.74E4	1.05E3
	$\Delta H_{\text{Me,Ads}}$ (kJ/mol)	Negligible	–
	$K^*_{\text{Me,Ads}}$ (m^3/mol)	9.11E−4	3.41E−5
	$\Delta H_{\text{Me,Ads}}$ (kJ/mol)	49.6	0.03
	$K^*_{\text{H}_2,\text{Des}}$ (mol/m^3)	1.61E2	7.55E−1
RDS model	E_A (kJ/mol)	114.4	0.02
	k_S^* (mol/m^3 s)	3.84E4	3.80E3
	$\Delta H_{\text{Me,Ads}}$ (kJ/mol)	Negligible	–
	$K^*_{\text{Me,Ads}}$ (m^3/mol)	1.14E−3	1.22E−4
	$\Delta H_{\text{H}_2,\text{Des}}$ (kJ/mol)	37.9	0.02
	$K^*_{\text{H}_2,\text{Des}}$ (mol/m^3)	1.50E2	0.82

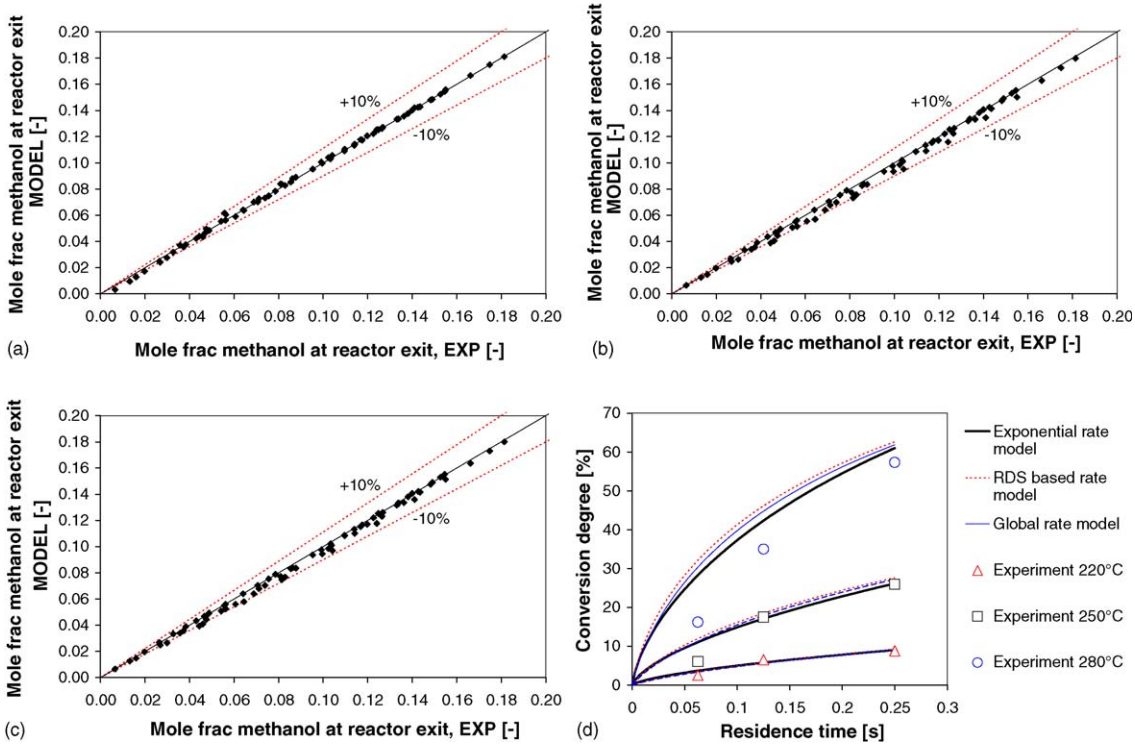

Fig. 7. Parity plots for (a) exponential rate model; (b) global rate model; (c) RDS based rate model and (d) comparison experimental and model data for the conversion degree as a function of residence time.

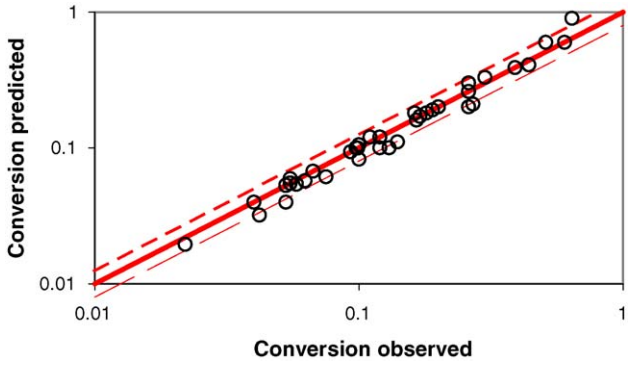

Fig. 8. Parity plot (on basis of methanol conversion degree) for experimental and global model data for the extrapolation into the pressure gap region (different partial and absolute pressures); dotted lines represent a relative deviation of 20%.

hydrogen addition to the reactant feed was not performed. This might result in a potential rate expression dependent on methanol and water concentration only.

Fig. 7a–c shows the parity plots for the different models applied and their good accordance in relation to the experimental data. Fig. 7d gives additional information about the residence time dependence of the conversion degree of the models compared to the experimental data of Fig. 3. There is no real significant difference between the data prediction of the models. The difference in the trend of the residence time-dependent experimental data to the model curve may be a result of the CO formation not included in the model or by an increase in experimental error when applying shorter microstructured foils (increase in bypass).

3.7. Model application to low pressure

The application of the derived kinetic model (global model) to the low-pressure experiments is an extrapolation of the parameter space with respect to the molar water to methanol ratio, reaction temperature and partial pressures of the compounds (see Section 2). Due to different deactivation observed in the two test rigs (see Section 2.1) the surface rate constant k_S had to be corrected by a factor 10^{-3} for the atmospheric pressure experiment (200 mbar partial pressure methanol). When applying this model to the other low-pressure experiments, it was found that the model describes the experimental results in the low pressure setup within a deviation of $\pm 20\%$ very well (Fig. 8). Including the elevated pressure experiments, the model covers a range of three decades in methanol partial pressure (0.6–736 mbar). It is a first hint that the mechanism does not change over this range of pressure values.

4. Conclusions

Boundary conditions were discussed in the present paper for data acquisition in microstructured reactors for kinetic modelling. Mass transfer limitations were excluded by appropriate methods, like varying diffusion coefficients and catalyst layer thickness.

Considering the reaction network of methanol steam reforming, of methanol decomposition and of reverse water gas shift reaction it was found that reforming is dominant and CO is produced by methanol decomposition in parallel. Water gas shift seems to be hindered in the reactant mixture. The CO sites seem to be located at the boundary of microstructured foil and catalysts. Oxidated PdZn at the reactor inlet is also a favourite CO production site.

Significant parameters for the methanol reforming are methanol and hydrogen partial pressure, the latter decreasing the reaction rate.

Considering experiments for determination of intermediate products of the reaction and rate-determining step it can be concluded that methyl formate is no intermediate on PdZn catalysts and C–H bond breakage (methoxy to formate) is rate determining from isotope labelled methanol experiments.

An exponential, a hyperbolic global and a rate-determining step based model were presented showing a good accordance to experimental data. Activation energies seem to be plausible and in agreement with calculated values and exponent similarities are partly given with copper systems. Model deviations to experimental values were very small highlighting the micro-channel reactor suitability for reaction modelling.

The extrapolation of the models to low-pressure experiments showed a good fit over a range of three decades in methanol partial pressure. Down to 0.6 mbar methanol pressure (30 mbar absolute pressure) no change in reaction mechanism can be detected.

Acknowledgement

For financial support of experiments in the pressure gap DFG FI816-1,2,3 is gratefully acknowledged.

References

[1] J.A. Christiansen, J. Am. Chem. Soc. 43 (1921) 1670.
[2] D.L. Trimm, Z.I. Önsan, Catal. Rev. 43 (2001) 31.
[3] N. Iwasa, N. Kudo, H. Takahashi, S. Masuda, N. Takezawa, Catal. Lett. 19 (1993) 211.
[4] P.S. Wehner, G.C. Tustin, B.L. Gustafson, J. Catal. 88 (1984) 246.
[5] Z. Zsoldos, A. Sárkány, L. Guczi, J. Catal. 145 (1994) 235.
[6] C.T. Hong, C.T. Yeh, F.H. Yu, Appl. Catal. 48 (1989) 385.
[7] V. Pour, J. Bartoň, A. Benda, Coll. Czech. Chem. Comm. 40 (1975) 2923.
[8] J. Bartoň, V. Pour, Coll. Czech. Chem. Comm. 45 (1980) 3402.
[9] E. Santacesaria, S. Carrà, Appl. Catal. 5 (1983) 345.
[10] J.C. Amphlett, M.J. Evans, R.A. Jones, R.F. Mann, R.D. Weir, Can. J. Chem. Eng. 63 (1985) 605.
[11] J. Agrell, H. Birgerson, M. Boutonnet, J. Power Sources 106 (2002) 249.
[12] K. Takahashi, N. Takezawa, H. Kobayashi, Appl. Catal. 2 (1982) 363.
[13] C.J. Jiang, D.L. Trimm, M.S. Wainwright, N.W. Cant, Appl. Catal. A 93 (1993) 245.
[14] C.J. Jiang, D.L. Trimm, M.S. Wainwright, N.W. Cant, Appl. Catal. A 97 (1993) 145.
[15] S.P. Tonner, D.L. Trimm, M.S. Wainwright, N.W. Cant, Ind. Eng. Chem. Res. Dev. 23 (1984) 384.
[16] B.A. Peppley, J.C. Amphlett, L.M. Kearns, R.F. Mann, Appl. Catal. A: Gen. 179 (1999) 31.

[17] K. Takahashi, H. Kobayashi, N. Takezawa, Chem. Lett. (1985) 759.
[18] P. Pfeifer, M. Fichtner, K. Schubert, M.A. Liauw, G. Emig, in: Proceedings of the Third International Conference on Microreaction Technology: Industrial Prospects, Frankfurt, 1999), p. 372.
[19] P. Pfeifer, K. Schubert, M.A. Liauw, G. Emig, Appl. Catal. A: Gen. 270 (2004) 165.
[20] P. Pfeifer, A. Wenka, K. Schubert, M.A. Liauw, G. Emig, AIChE J. 50 (2004) 418.
[21] A. Kölbl, P. Pfeifer, M. Fichtner, M. Kraut, K. Schubert, M.A. Liauw, G. Emig, Chem. Eng. Technol. 27 (6) (2004) 671.
[22] P. Pfeifer, K. Schubert, M.A. Liauw, G. Emig, Trans. IChemE 81 (2003) 711.
[23] G.J. Taylor, Proc. R. Soc. London 223A (1954) 446.
[24] R. Aris, Proc. R. Soc. London 235A (1956) 67.
[25] P. Pfeifer, PhD, University Erlangen-Nuremberg, 2003.
[26] N. Takezawa, N. Iwasa, Catal. Today 36 (1997) 45.
[27] Z.-X. Chen, K.N. Neymann, A.B. Gordienko, N. Rösch, Phys. Rev. B 68 (2003) 1.
[28] Z.-X. Chen, K.M. Neyman, K.H. Lim, N. Rösch, Langmuir 20 (2004) 8068.
[29] Z.-X. Chen, K.H. Lim, K.M. Neyman, N. Rösch, Phys. Chem. Chem. Phys. 6 (2004) 4499.
[30] J.K. Lee, J.B. Ko, D.H. Kim, Appl. Cat. A 278 (2004) 25–35.
[31] H. Purnama, T. Ressler, R.E. Jentoft, H. Soerijanto, R. Schlögl, R. Schomäcker, Appl. Cat. A 259 (2003) 83.
[32] S.R. Samms, R.F. Savinell, J. Power Sources 112 (2002) 13.
[33] C. Cao, G. Xia, J. Holladay, E. Jones, Y. Wang, Appl. Cat. A 262 (2004) 19–29.